



## **Thermally re-distributed IRSL (RD-IRSL): A new possibility of dating sediments near B/M boundary**

**Morthekai, P.; Chauhan, P.R. ; Jain, Mayank; Shukla, A.D. ; Rajapara, H.M. ; Krishnan, K. ; Sant, D.A. ; Patnaik, R. ; Reddy, D.V. ; Singhvi, A.K.**

*Published in:*  
Quaternary Geochronology

*Link to article, DOI:*  
[10.1016/j.quageo.2015.05.018](https://doi.org/10.1016/j.quageo.2015.05.018)

*Publication date:*  
2015

*Document Version*  
Peer reviewed version

[Link back to DTU Orbit](#)

*Citation (APA):*  
Morthekai, P., Chauhan, P. R., Jain, M., Shukla, A. D., Rajapara, H. M., Krishnan, K., Sant, D. A., Patnaik, R., Reddy, D. V., & Singhvi, A. K. (2015). Thermally re-distributed IRSL (RD-IRSL): A new possibility of dating sediments near B/M boundary. *Quaternary Geochronology*, 30(Part B), 154–160.  
<https://doi.org/10.1016/j.quageo.2015.05.018>

---

### **General rights**

Copyright and moral rights for the publications made accessible in the public portal are retained by the authors and/or other copyright owners and it is a condition of accessing publications that users recognise and abide by the legal requirements associated with these rights.

- Users may download and print one copy of any publication from the public portal for the purpose of private study or research.
- You may not further distribute the material or use it for any profit-making activity or commercial gain
- You may freely distribute the URL identifying the publication in the public portal

If you believe that this document breaches copyright please contact us providing details, and we will remove access to the work immediately and investigate your claim.

# Thermally re-distributed IRSL (RD-IRSL): A new possibility of dating sediments near B/M Boundary

P. Morthekai<sup>1\*</sup>, P. R. Chauhan<sup>2</sup>, M. Jain<sup>3</sup>, A. D. Shukla<sup>4</sup>, H. M. Rajapara<sup>4</sup>, K. Krishnan<sup>5</sup>, D. A. Sant<sup>6</sup>, R. Patnaik<sup>7</sup>, D. V. Reddy<sup>8</sup>, A. K. Singhvi<sup>4</sup>

<sup>1</sup>*Luminescence Dating Laboratory, Birbal Sahni Institute of Palaeobotany, Lucknow – 226 007, India.*

<sup>2</sup>*Department of Humanities and Social Sciences, Indian Institute of Science Education and Research, Mohali - 140306, India.*

<sup>3</sup>*Centre for Nuclear Technologies, Risoe-DTU, 4000 Roskilde, Denmark.*

<sup>4</sup>*Geosciences Division, Physical Research Laboratory, Navrangpura, Ahmedabad – 380 009, India.*

<sup>5</sup>*Department of Archaeology and Ancient History, Faculty of Arts, The Maharaja Sayajirao University of Baroda, Vadodara – 390 002, India.*

<sup>6</sup>*Department of Geology, Faculty of Science, The Maharaja Sayajirao University of Baroda, Vadodara – 390 002, India.*

<sup>7</sup>*Centre of Advanced study in Geology, Panjab University, Chandigarh - 160014, India.*

<sup>8</sup>*CSIR-National Geophysical Research Institute, Uppal Road, Hyderabad – 500 007, India.*

\* Corresponding author: morthekai@gmail.com

This study attempted to probe a geologically more stable IR stimulated luminescence signal (IRSL) that explored so far. IRSL, probes the proximal pairs and, pIRSL measurements at elevated temperatures consume more distant pairs. We surmised that the residual IRSL after pIR-IRSL should arise from most distant pairs and hence should be more stable. A thermal stimulation after pIR-IRSL leads to redistribution of charges including distant pairs and this can be probed by further IRSL and pIRSL (post IR IRSL) measurements. This post IRSL following a thermal treatment is termed as redistributed IRSLs (RD IRSL and RD pIRSL) and contributes about 10% of total IRSL counts from a pristine sample. As expected, RD IRSL has a poor to be solar bleachability. Burial age of around 800 ka (with 30 - 40 %) using RD-IRSL and RD-pIRSL were comparable with the palaeomagnetic dating and were a factor of three higher than conventional pIR-IRSL, TRL, IR-RL and VSL ages.

**Keywords:** IRSL dating; Feldspar dating; VSL; post IR IRSL; Dhansi Formation

## **Introduction**

Infra-red stimulated luminescence signals (IRSL), which are unique to the feldspars, have a complex production mechanism but on account of a higher saturation dose, have the potential to date older sediments (Hutt et al., 1988, Jain and Ankjaergaard, 2011, Buylaert et al., 2012, Morthekai et al., 2011, Biswas et al., 2013). A large variety of IRSL signals can be obtained by changing the thermo-optical pre-treatments or/and by varying the sample temperatures (Poolton, 2009, Morthekai et al., 2012, Pagonis et al., 2012). Considerable efforts have been made to understand the production mechanism of IRSL and some consistency in the understanding has been achieved (Jain and Ankjaergaard, 2011, Kars et al., 2013; Jain et al. 2015). It has been earlier debated whether IRSL and pIRIR signals arise from single-trap or multi-traps (Thomsen et al., 2011); based on spectroscopic measurements Andersen et al., (2012) concluded that both IRSL and pIRIR signals arise from the same trap. In this scenario, pIRSL signals (post IR IRSL), that are measured after a low temperature IRSL readout on a preheated sample, arise from recombination of distant pairs of trapped charges rather than from deeper/stable traps; the higher the IR stimulation temperature the greater the access to distant pairs. The limiting temperature though for IR stimulation is the preheat temperature. It is reasonable to assume that even more stable distant trapped electron-hole pairs compared to the individual IRSL and pIRIR measurements, are available in the feldspar grains after IRSL and pIRSL measurements are completed. It will be shown that such remaining pairs can be re-distributed by a thermal treatment and re-distributed trapped electrons can be measured with relatively lower temperature IRSL measurements. The present study aimed to 1) measure distant pairs of trapped charges by re-distributing them by thermal perturbation and 2) check the suitability of this signal for palaeodose estimation by using old samples with independent age controls. Age estimates using other optical variants were also measured for the same sample and were found to be a factor of 2-3 lower.

## **Sample Selection**

The samples are from the Dhansi Formation in Narmada Basin (Dhansi village in Hoshangabad district: 22° 47" N; 77° 37" E), central India which is dated to be older than 0.78 Ma (Rao et al.,

1997) with associated archaeological evidence that additionally attested to their antiquity (Patnaik et al., 2009). Rao et al. (1997) carried out paleomagnetic studies at multiple stratigraphic sections in the central and eastern part of the Narmada Basin in Madhya Pradesh. Samples were collected from stratigraphic contexts at Baneta, Hirdepur, Devkachar, Hathnora, Surajkund, Burhi Narmada and Pawla and Gurwara areas, all of which resulted in normal polarity. Only the samples from the section at Dhansi showed reversed magnetic polarity (Fig. 1) and samples from Chorbareta suggests the preservation of the Reversed to Normal polarity transition. In that respect, the Dhansi section is interpreted to be older than 0.73 Ma<sup>1</sup> while the remaining sections are younger than the Early Pleistocene. The section at Dhansi was sampled by Rao and colleagues (1997) for paleomagnetic data as it was stratigraphically below the Middle Pleistocene Surajkund Formation. In their study, Rao et al. (1997) followed standard paleomagnetic sample collection procedures following section cleaning and logging. Ninety-five samples of approximately 2.5 cm each were collected, prepared and processed using a Schonstedt-make spinner magnetometer (DSM2) following successive demagnetization by thermal and AF methods. At the time of their publication, no stone tools were observed eroding from the section. That discovery was made much later and formally reported by Patnaik et al. (2009). Therefore, the paleoanthropological significance of the ~15m Dhansi type-section is two-fold. It represents the longest and oldest (as currently known) Pleistocene stratigraphic sequence in the whole of central India and has yielded the first-known unequivocal Early Pleistocene stone tools in the region. While the artifacts and associated sediments are still under various scientific analyses, the preliminary dating results by Rao et al. (1997) will be confirmed through further paleomagnetic studies (at a higher sampling resolution) by the Narmada Basin Paleoanthropology Project. It is also hoped the new paleomagnetic study results will be combined with results from other applicable dating methods such as cosmogenic nuclide dating as well as the luminescence dating attempt represented by this paper.

Four samples (DNS OSL P-1, DNS OSL P-N, DNS OSL P-3 and DNS OSL P-4) were collected above (100 and 35 cms) and below (100 and 210 cms) below the horizon that yielded lower

---

<sup>1</sup>Today the global transition from Matuyama to Brunhes polarity is dated to 0.78 Ma. Although it is not impossible for the Dhansi Formation to represent an *older* Reversed polarity stage (because the Matuyama-Brunhes transition is not stratigraphically preserved here), we are currently assuming it belongs primarily to the Matuyama.

palaeolithic artifacts (Fig. 1). Standardsampling procedures were used. The samples were chemically treated with 1 N HCl and 40 %  $\text{H}_2\text{O}_2$  to remove carbonates and organic materials respectively. The 90 – 250  $\mu\text{m}$  grain size fractions from each sample were obtained by dry sieving. Quartz and non-quartz grains were extracted using isodynamic barrier magnetic separator (LB Frantz Magnetic Separator). From the non-quartz grains, K-feldspar grains were extracted using sodium poly-tungstate (heavy liquid) by exploiting the density difference between K-feldspars ( $< 2.58 \text{ g/cc}$ ) and others. No effort has been made to extract other feldspar portions (Na- or Ca-feldspars) other than K-feldspars. Quartz and feldspar grains were etched using 40 % HF and 10 % HF respectively for 80 minutes followed by HCl treatment (12 N). Grains which are smaller than 90  $\mu\text{m}$  were discarded by wet sieving. The sample preparations were carried out in National Geophysical Research Institute (NGRI), Hyderabad, India and Physical Research Laboratory (PRL), Ahmedabad, India.

The purity of quartz grains were confirmed from the near background IRSL counts from the quartz extraction. Feldspar grains ( $\sim 6000$  grains) were mounted in stainless steel discs in monolayer using silicon oil spray. The luminescence measurements were carried out in Risø TL/OSL Reader TA-20 (Bøtter-Jensen et al., 2003; Lapp et al., 2009) that is equipped with blue (LEDs:  $470 \pm 30 \text{ nm}$ ; filtered through GG-420 long-pass filter) and IR (LEDs:  $870 \pm 40 \text{ nm}$ ) stimulation sources both in continuous and pulse mode of stimulations. IRSL signals were detected by a photomultiplier tube (EMI 9235QA) through the combination of the filters BG 39 (2 mm thickness) and Corning 5-79 (4 mm). OSL (blue light stimulated luminescence) signals were detected through a 7.5 mm of Hoya U-340 filter. A calibrated beta sources ( $^{90}\text{Sr}/^{90}\text{Y}$ ) delivering  $0.12 \text{ Gy.s}^{-1}$  was used to irradiate the samples in the reader. The heating rate was  $2^\circ\text{C/s}$  and the heating was done in an ultrapure nitrogen gas atmosphere. VSL measurements were done following the protocol of Ankjærgaard et al. (2014). All the luminescence measurements were carried out from PRL, Ahmedabad except VSL which was carried out in Risø-DTU, Roskilde, Denmark. DNS OSL P-4 was measured in Birbal Sahni Institute of Palaeobotany, Lucknow, India.

Dose rates were estimated from the natural radioactive elements of U, Th and K in the sediment. U, Th and K from DNS OSL P-1, P-3 and P-4 were estimated using NaI:TI based gamma

spectrometer (Chiozzi et al., 2000) and that from DNS OSL P-N were measured using high pure Ge (HPGe) based gamma spectrometer (Shukla et al., 2002). These measurements were carried out from NGRI and PRL, India respectively and the values are tabulated in Table 1. Water content of the samples were assumed to  $5 \pm 2$  % for DNS OSL P-1 and P-N and  $10 \pm 5$  % for DNS OSL P-3 and P-4. The internal K in feldspar grains was assumed to be  $13.5 \pm 0.5$  %. The cosmic ray dose rate was calculated using an empirical relationship (Prescott and Hutton, 1994) and an average cosmic ray dose rate of  $1.19 \mu\text{Gy} \cdot \text{a}^{-1}$  was used.

### **Dose estimation using other signals**

The burial doses of feldspar grains were estimated using pIRSL@290°C (Thiel, et al., 2012), MET-pIRSL (Li and Li, 2012), Time resolved luminescence, TR-IRSL (Jain et al., 2014) and IR-RL (Buylaert et al., 2012) signals. And that of quartz grains were estimated using VSL (Jain 2009; Ankjaergaard et al., 2015) and thermal transferred OSL, TT-OSL (Duller and Wintle, 2012). These studies reported that these signals to be stable and hence appropriate for dating of samples at, and beyond the Brunhes-Matuyama Boundary,  $> 780$  ka.

*Post IR IRSL:* pIRSL@290°C was measured for 200 s after an IRSL readout at 50°C and with a preheat of 320°C. The SAR procedure was employed for  $D_e$  estimation (Murray and Wintle, 2003). The estimated ages of DNS OSL P-1 using IRSL (at 50°C) and post IR IRSL (at 290°C) were  $148 \pm 20$  and  $367 \pm 86$  ka. The values are the arithmetic average and standard deviation of two aliquots.

*MET-pIRSL:* Subsequent pIRSL@T°C where T varied from 100°C to 300°C were measured for 100 s after an IRSL readout at 50°C and with a preheat of 320°C. Before every regeneration dose administration, the remnant luminescence signals were removed by thermo-optical wash using IR at 325°C for 100 s. The SAR procedure was employed for  $D_e$  estimation using each pIRSL signal. The estimated ages of DNS OSL P-1 using post IR IRSL (at T°C; 100 – 300 at 50°C interval) were varying from  $285 \pm 80$  (at 100°C) to  $570 \pm 240$  ka (at 300°C). The values are the arithmetic average and standard deviation of two aliquots.

*TRL*: Time resolved luminescence signals were measured using pulsed IR stimulation at 50°C with 50  $\mu$ s ON time and 500  $\mu$ s OFF time. The photon arrival times were detected using a Photon Timer attachment (Lapp et al., 2009). Total stimulation time was 2000 s and hence  $\sim$  3.6 million pulses with a pulse period of 550  $\mu$ s were used. SAR procedure was used to estimate the equivalent dose ( $D_e$ ) with a preheat temperature of 250°C and an IR bleaching step (100 s at 220°C) before every regeneration dose administration (Jain et al., 2014). Integral IRSL counts from 0-50  $\mu$ s, 50.1 – 100  $\mu$ s, 100.1 – 200  $\mu$ s, 200.1 – 300  $\mu$ s and 300.1 – 500  $\mu$ s of photon arrival times were used in  $D_e$  calculation. The dose response curves were fitted to single saturating exponential function and the estimated ages DNS OSL P-1 are  $120 \pm 25$  ( $630 \pm 50$ ),  $170 \pm 40$  ( $570 \pm 50$ ),  $170 \pm 40$  ( $570 \pm 50$ ),  $140 \pm 30$  ( $660 \pm 50$ ) and  $140 \pm 30$  ( $670 \pm 50$ ) ka respectively. Values in parentheses are  $D_0$  in Gy. The late arrival photons would have been the result of recombination of distant pairs of trapped charges and hence considered to be more stable giving higher burial dose. Although the  $D_e$  values from the OFF period are similar within the error limit, there is a systematic lowering of  $D_e$  towards late photon arrival time integration which is opposite to the anticipation. However this is the result from one aliquot.

*IR-RL*: Natural and laboratory induced IR-RL signals were measured for 5000 s and 40,000 s respectively and were compared to estimate the  $D_e$ ; however no sensitivity correction was employed (Buylaert et al., 2012, Varma et al., 2013). Before the regeneration dose was administered all the trapped electrons were emptied by illuminating the grains to UV light for 800 s. The average (of three aliquots)  $D_e$  and estimated age for DNS OSL P-1 are  $570 \pm 80$  Gy and  $240 \pm 20$  ka respectively.

*VSL*: Violet stimulated luminescence (VSL) involves 402 nm photons stimulation at room temperature, with the emission detected using a PMT equipped with the filter combination of 7.5 mm Hoya U-340, 2 mm GG 395 and a laser clean up filter (Semrock LD01-405/10; Jain, 2009). This set up is available in the above mentioned Risø Reader type (DA-20) and the beta dose rate was  $0.0485 \text{ Gy.s}^{-1}$ . VSL signals from quartz extraction were measured following the modified SAR protocol as suggested by Ankjaergaard et al. (2015) where the sample is preheated to

300°C/100 s (at 5°C/s) and bleached by blue LEDs for 100 s at 125°C before it was measured VSL (402 nm stimulation) for 100 s at 30°C. The residual signals are bleached by illuminating the grains to violet laser diode for 280 s at 280°C. Background subtracted integrated VSL signals from 0 – 3 s (BKG: average of 3 – 10.5 s) and from 9 – 29 s (BKG: average of 29 – 80 s) were considered to be Component A and Component B respectively (Ankjaergaard et al., 2013). The constructed dose response curves were fitted to double saturating exponential functions and the ages estimated using Component A are  $370 \pm 110$  ( $1010 \pm 680$  Gy),  $330 \pm 100$  ( $9100 \pm 12000$  Gy) and  $210 \pm 90$ ka ( $760 \pm 270$  Gy) for DNS OSL P-1, DNS OSL P-N and DNS OSL P-3 samples respectively and second saturation dose,  $D_{o,2}$ , values are in parentheses. These values are the arithmetic mean and standard deviation of the 3 aliquots (2 aliquots for DNS OSL P-3) for each sample. The test dose error was restricted to 10 % and the recycling point and the recuperation were within 15 and 10 % respectively. Component B exhibited higher recuperation dose (~ 20 %) and hence it was not considered for  $D_e$  estimation.

*TT-OSL*: OSL signals were measured after the quartz grains were preheated to 260°C for 10 s. Further, the thermally transferred OSL was measured after a preheat upto 260°C for 10 s and there was a thermo-optical wash at 300°C for 200 s before every regeneration dose (Stevens et al., 2009; Hernandez et al., 2012). Only one aliquot was measured and the age of DNS OSL P-1 is  $250 \pm 80$ ka.

### **Re-distributed IRSL**

The distant trapped charge pairs left after IRSL and pIRSL measurements were probed by the protocol outlined in figure 2. According to this procedure, the IRSL is measured at 300°C for 100 s on a preheated sample upto the temperature of 360°C. Subsequently, another IRSL at 320°C was measured for 500 s and it is called pIRSL. The temperature and IR stimulation time were optimized based on the maximum luminescence output and removal of conventional IRSL signals (Fig. 1S, Fig. 2Sa,b,c). The previous IRSL and pIRSL measurements would have consumed the proximal pairs and left the distant pairs untouched. These distant pairs were possibly re-distributed by thermal perturbation by heating upto 450°C and this temperature was



optimized by making sure that there were no TL signals from the TL peak at  $\sim 410^{\circ}\text{C}$  (Fig. 1S, Fig. 2Sc). Thus re-distributed pairs were probed by another set of IRSL and pIRSL measurements and they are named as re-distributed IRSL (RD-IRSL) and re-distributed pIRSL (RD-pIRSL) signals. Both the re-distributed IRSL signals approximately contributed to 10 % of the total IRSL counts (Fig. 3). Before the test dose was administered, the system (feldspar grains) was cleaned by IR illumination for 500 s at the temperature of  $400^{\circ}\text{C}$ .

The distant pairs are expected to be stable and not necessarily easy-to-bleach by under daylight during transportation. A maximum of 6 hours solar bleaching (solar simulator after cutting the UV component) was employed on different aliquots of DNS OSL P-3. Both pIRSL and RD-IRSL showed a similar bleaching behavior where there was a maximum unbleached dose for the solar bleaching time of 1 minute and then a monotonous decay (Fig. 4a). Unbleached dose (arithmetic average of 3 aliquots) after 6 hours of solar simulator in DNS OSL P-1 shows an increase from IRSL to RD-pIRSL signals. However the standard deviation is very large for RD-IRSL signal (inset of Fig. 4a). IRSL measured at  $300^{\circ}\text{C}$  showed a monotonous decay with the bleaching time. Standardized growth curves (SGC) were constructed using IRSL, pIRSL, RD-IRSL and RD-pIRSL signals and are shown in Fig. 4b. The growth curves for RD-IRSL and RD-pIRSL are similar. However, SGCs of pIRSL, RD-IRSL and RD-pIRSL signal are 1.17, 2.21 and 2.28 times that of IRSL, respectively (inset of Fig. 4b). Re-distributed signals have similar bleaching characteristics and dose response curves than those of IRSL and pIRSL signals. These could be explained by either with multi-trap system or with donor-acceptor distance distribution (with single trap system). However, the presence of multi-traps are not seen in the TL curves (after preheat to  $360^{\circ}\text{C}$ ) with different heating rates ( $0.1^{\circ}\text{C.s}^{-1}$ ,  $1^{\circ}\text{C.s}^{-1}$  and  $10^{\circ}\text{C.s}^{-1}$ ) as there were no TL peaks in higher temperature region after  $\sim 500^{\circ}\text{C}$  (Fig. 1S). So, these re-distributed signals can be attributed to be arising from the far distant pairs assuming a single trap model.

Dose recovery tests were performed on the bleached aliquots (3 aliquots) under the solar simulator for 6 hours. The unbleached dose from these 3 aliquots were measured using SAR protocol and found that the re-distributed IRSL signals were also bleached to a residual level (Fig. 5a) but with a large spread. Two sets of laboratory doses (220 Gy and 1100 Gy) were given to these bleached aliquots of DNS OSL P-1. These two sets of doses were reproduced with an

underestimation of 10-15 % and the lower dose (220 Gy) was reproduced better than higher dose (1100 Gy) (Fig. 5b). Fading rates were measured (from 3 aliquots; Fig. 6a; Auclair et al., 2003) and it was observed that both the re-distributed signals exhibit near zero fading but with large spread in the fading rates (Fig. 6c).

The burial dose was estimated using all the four signals (IRSL, pIRSL, RD-IRSL and RD-pIRSL) following SAR procedure. For IRSL and RD-IRSL, the background subtracted (average of last 20 s signals) integral counts of first 4 s were used. The signal-to-background ratio for pIRSL and RD-pIRSL were 20:95 s and 40:95 s respectively. The recycling ratio and test dose error were within 15 and 10 % respectively and the recuperation was also within 10 %. It was observed that pIRSL suffered with large test dose error (more than 10 %) and there was a high ITL during pIRSL measurement. RD-pIRSL signals were in field-saturation in many aliquots whereas IRSL signals were having  $83 \pm 3$  % of field saturated dose and RD-IRSL signals had  $90 \pm 10$  %. Six aliquots were measured from each sample (12 aliquots for DNS OSL P-4).

## Discussion

The estimated ages using all the mentioned signals are plotted (Fig. 7). DNS OSL P-1 has age estimates from all the signals. Except re-distributed IRSL signals (RD-IRSL and RD-pIRSL), all else showed underestimation. However, the upper bound of MET-pIRSL derived age also could reach to the B/M boundary. Although the dose response curves of both the re-distributed IRSL signals (RD-IRSL and RD-pIRSL) are similar, natural RD-pIRSL signals were in saturation. The reason for this could be the relatively higher natural RD-pIRSL signals than RD-IRSL (data not shown). The relatively poor bleachability of RD-pIRSL signals would have left more unbleached dose (and hence the RD-pIRSL signal) which would have hindered interpolation into the dose response curve.

With this small data set, it is not possible to conclude that pIRSL@290°C, TRL, IR-RL, VSL and TT-OSL can't be used to date this older materials. But certainly it can be inferred that re-distributed IRSL signals, particularly RD-IRSL, have the potential to date the samples around the B/M boundary considering the good luminescence characteristics of this signal (Figs. 4-6).

The age estimates of DNS OSL P-1 and DNS OSL P-4 are near the B/M boundary within the uncertainty. But those of DNS OSL P-N and DSN OSL P-3 are smaller than the sample from the upper strata (DNS OSL P-1) and is against the principle of superposition. There is a pattern in the age estimates that (DNS OSL)  $P-4 > P-1 > P-N > P-3$  and this is seen for the re-distributed IRSL signals (Fig. 7). This is not only among the re-distributed IRSL signals from feldspars, but also can be seen in VSL age estimates of quartz (except P-4 which has not been done using VSL). This can be possibly understood with the on-going multi-disciplinary studies (including palaeomagnetism, cosmo-genic radio-nuclide and geochemistry) on this section and perhaps requires a more careful assessment of the long term dose rates of the individual samples.

## **Conclusion**

Two new signals named as re-distributed infra-red stimulated luminescence (RD-IRSL and RD-pIRSL) and have been investigated for their potential to increase the age range. These signals are induced by a thermal perturbation (heating upto 450°C) after IRSL/pIRSL measurement, and are considered to arise from the distant trapped charge pairs in the irradiated feldspar crystal. Our preliminary investigations suggest that these signals have sufficient intensity (10% of the first IRSL) and acceptable dosimetric characteristics. The dating results ( $900 \pm 360$  and  $850 \pm 230$  ka for DNS OSL P-1;  $770 \pm 265$  ka and  $970 \pm 290$  ka for DNS OSL P-4, using RD-IRSL and RD-pIRSL signals respectively) from samples around the Bruhnes-Matuyama palaeomagnetic reversal in central India are highly encouraging.

## **Acknowledgements**

Dr. Manoj Rathore from MPCOST, Ms. Vaidehi from PRL are acknowledged for their kind help during luminescence measurements. International Travel Support of DST, India and CICS, Chennai are acknowledged for the travel support and accommodation support respectively to participate and present this work in 14<sup>th</sup> LED 2014, Montreal, Canada. We thank the Archaeological Survey of India for the field permit and the Wenner-Gren Foundation for Anthropological Research for funding this project (Grant 8367 awarded to PRC). PRC also

thanks the Director, IISER for academic support of the research. We acknowledge the reviewer's remarks and efforts to improve the quality of this research article.

### **Figure Captions:**

Fig. 1a) Location of the sampling site. b) A comparison of the palaeomagnetic results of samples from the Middle Pleistocene Surajkund Formation and Early Pleistocene Dhansi Formation (modified from Rao et al. 1997).

Fig. 2. Protocol for measuring the distant pairs.

Fig. 3. Four variants of IRSL signals measured in the protocol as given in Fig. 2.

Fig. 4.a) Bleachability curves of DNS OSL P-3 and b) standardized growth curves of the four IRSL variants of DNS OSL P-1.

Fig. 5.a) Residual unbleached dose after 6 hour solar bleaching using solar simulator and b) dose recovery tests performed using two sets of laboratory doses on DNS OSL P-1.

Fig. 6.a) Fading rates measurement on DNS OSL P-1 and b) compilation of the fading rates.

Fig. 7. Age estimates using the luminescence signals discussed in the text. The hyphenated line indicates the B/M boundary.

Fig. 1S. TL measured upto 700°C (data shown till 650°C) with different heating rates (legends).

Fig. 2S. Optimization of the timing and temperature to measure the redistributed IRSL signals.

### **References**

1. Aitken, M. J., 1985. Thermoluminescence dating. Academic Press, London.
2. Andersen, M. T., Jain, M., Tidemand-Lichtenberg, P., 2012. 'Red-IR stimulated luminescence in K-feldspar: Single or multiple trap origin?'. Journal of Applied Physics 112, 043507pp.
3. Ankjaergaard, C., Jain, M., Wallinga, J., 2013. Towards dating Quaternary sediments using the quartz Violet stimulated luminescence (VSL) signal. Quaternary Geochronology 18, 99-109.

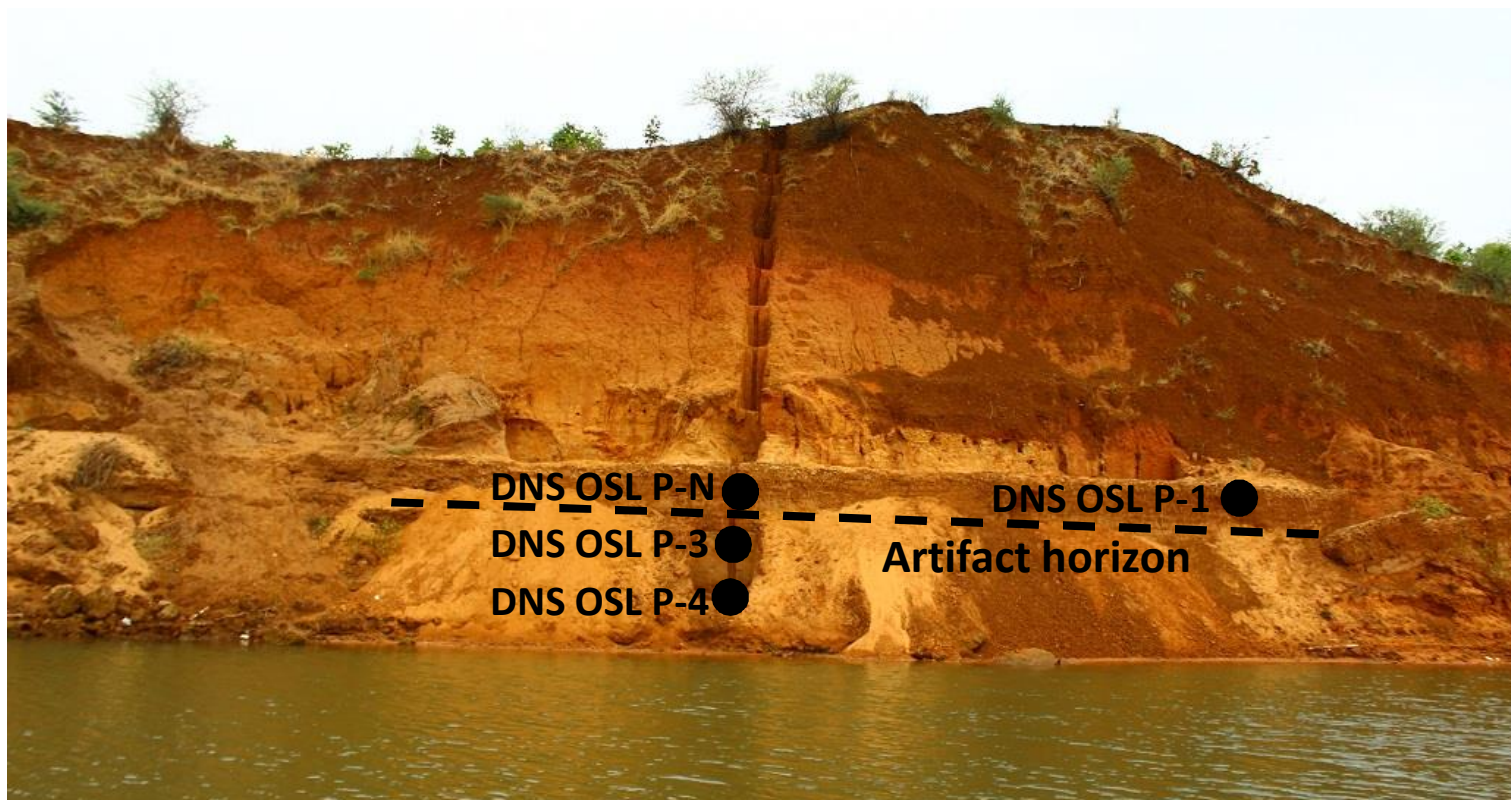
4. Ankjaergaard, C., Guralnik, B., Porat, N., Heimann, A., Jain, M. and Wallinga, J., 2015. Violet stimulated luminescence: geo- or thermochronometer? *Radiation Measurements*, *accepted*.
5. Auclair, M., Lamothe, M. and Huot, S., 2003. Measurement of anomalous fading for feldspar IRSL using SAR. *Radiation Measurements* 37, 487-492.
6. Biswas, R. H., Williams, M. A. J., Raj, R., Juyal, N., Singhvi, A. K., 2013. Methodological studies on luminescence dating of volcanic ashes. *Quaternary Geochronology* 17, 14-25.
7. Boetter-Jensen, L., Andersen, C. E., Duller, G. A. T., Murray, A. S., 2003. Developments in radiation, stimulation and observation facilities in luminescence measurements. *Radiation Measurements* 37, 535-541.
8. Buylaert, J. P., Jain, M., Murray, A. S., Thomsen, K. J., Thiel, C., Sohbati, R., 2012. A robust feldspar luminescence dating method for Middle and Late Pleistocene sediments. *Boreas* 41, 435-451.
9. Buylaert, J. P., Jain, M., Murray, A. S., Thomsen, K. J., Lapp, T., 2012. IR-RF dating of sand-sized K-feldspar extracts: a test of accuracy. *Radiation Measurements* 47, 759-765.
10. Chiozzi, P., De Felice, P., Fazio, A., Pasquale, V., Verdoya, M., 2000. Laboratory application of NaI(Tl)  $\gamma$ -ray spectrometry to studies of natural radioactivity in geophysics. *Applied Radiation and Isotopes* 53, 127-132.
11. Duller, G. A. T. and Wintle, A. G., 2012. A review of the thermally transferred optically stimulated luminescence signal from quartz for dating sediments. *Quaternary Geochronology* 7, 6-20.
12. Henandez, M., Mauz, B., Mercier, N. and Shen, Zhixiong, 2012. Evaluating the efficiency of TT-OSL SAR protocols. *Radiation Measurements* 47, 669-673.
13. Hutt, G., Jaek, I., Tchonka, J., 1988. Optical dating: K-feldspars optical response stimulation spectra. *Quaternary Sciences Reivews* 7, 381-385.
14. Jain, M., 2009. Extending the dose range: Probing deep traps in quartz with 3.06 eV photons. *Radiation Measurements* 44, 445-452.
15. Jain, M., Ankjaergaard, C., 2011. Towards a non-fading signal in feldspar: Insight into charge transport and tunneling from time-resolved optically stimulated luminescence. *Radiation Measurements* 46, 292-309.

16. Jain, M., Buylaert, J. P., Thomsen, K. J., Murray, A. S., 2014. Further investigations on 'non-fading' in K-feldspar. *Quaternary International*, under Review.
17. Jain, M., Sohbati, R., Guralnik, B, Murray, A. S., Kook, M., Lapp, T., Prasad, A. K., Thomsen, K. J. and Buylaert, J. P., 2015. Kinetics of infra-red stimulated luminescence from feldspars. *Radiation Measurements*, *Accepted*.
18. Kars, R. H., Poolton, N. R. J., Jain, M., Ankjaergaard, C., Dorenbos, P., Wallinga, J., 2013. On the trap depth of the IR-sensitive trap in Na- and K-feldspar. *Radiation Measurements* 59, 103-113.
19. Lapp, T., Jain, M., Ankjaergaard, C., Pitzel, L., 2009. Development of pulsed stimulation and photon timer attachments to the Risoe TL/OSL reader. *Radiation Measurements* 44, 571-575.
20. Li, B. and Li, S. H., 2012. Luminescence dating of Chinese loess beyond 130 ka using the non-fading signal from K-feldspar. *Quaternary Geochronology* 10, 24-31.
21. Morthekai, P., Jain, M., Cunha, P. P., Azevedo, J. M., Singhvi, A. K., 2011. An attempt to correct for the fading in million year old basaltic rocks. *Geochronometria* 38, 223-230.
22. Morthekai, P., Jugina Thomas, Pandian, M. S., Balaram, V., Singhvi, A. K., 2012. Variable range hopping mechanism in band-tail states of feldspars: A time-resolved IRSL study. *Radiation Measurements* 47, 857-863.
23. Murray, A. S., Wintle, A. G., 2003. The single aliquot regenerative dose protocol: potential for improvements in reliability. *Radiation Measurements* 37, 377-381.
24. Pagonis, V., Jain, M., Murray, A. S., Ankjaergaard, C., Chen, R., 2012. Modeling of the shape of infrared stimulated luminescence signals in feldspars. *Radiation Measurements* 47, 870-876.
25. Patnaik, R., Chauhan, P. R., Rao, M. R., Blackwell, B. A. B., Skinner, A. R., Sahni, A., Chauhan, M. S., Khan, H. S., 2009. New geochronological, palaeoclimatological, and archaeological data from the Narmada Valley hominin locality, central India. *Journal of Human Evolution* 56, 114-133.
26. Poolton, N. R. J., Kars, R. H., Wallinga, J., Bos, J. J., 2009. Direct evidence for the participation of band-tails and excited-state tunneling in the luminescence of irradiated feldspars. *Journal of Physics: Condensed Matter* 21, 485505-485515.

27. Prescott, J. R., Hutton, J. T., 1994. Cosmic ray contributions to dose rates for luminescence and ESR dating: large depths and long-term time variations. *Radiation Measurements* 23, 497-500.
28. Rao, V. K., Chakroborti, S., Rao, K.J., Ramani, M.S.V., Marathe, S.D., Borkar, B.T., 1997 Quaternary geology of the Narmada valley: a multidisciplinary approach. *Special Publications of Geological Survey of India* 46, 65-78.
29. Shukla, A. D, Bhandari, N and Shukla, P. N., 2002. The chemical signatures of the Permian-Triassic transitional Environment in Spiti Valley, India. *Proceedings of Catastrophic Events and Mass Extinction: Impacts and Beyond, Geological Society of America (Special Paper)* 356, 445-454.
30. Stevens, T., Buylaert, J. P. and Murray, A. S., 2009. Towards development of a broadly-applicable SAR TT-OSL dating protocol for quartz. *Radiation Measurements* 44, 639-645.
31. Thiel, C., Buylaert, J. P., Murray, A. S., Elmedjoub, N., Jedoui, Y., 2012. A comparison of TT-OSL and post-IR IRSL dating of coastal deposits on Cap Bon peninsula, north-eastern Tunisia. *Quaternary Geochronology* 10, 209-217.
32. Thomsen, K. J., Murray, A. S., Jain, M., 2011. Stability of IRSL signals from sedimentary K-feldspar samples. *Geochronometria* 38, 1-13.
33. Varma, V., Biswas, R. H., Singhvi, A., 2013. Aspects of infrared radioluminescence dosimetry in K-feldspar. *Geochronometria* 40, 266-273.

Fig. 1

a)



b)

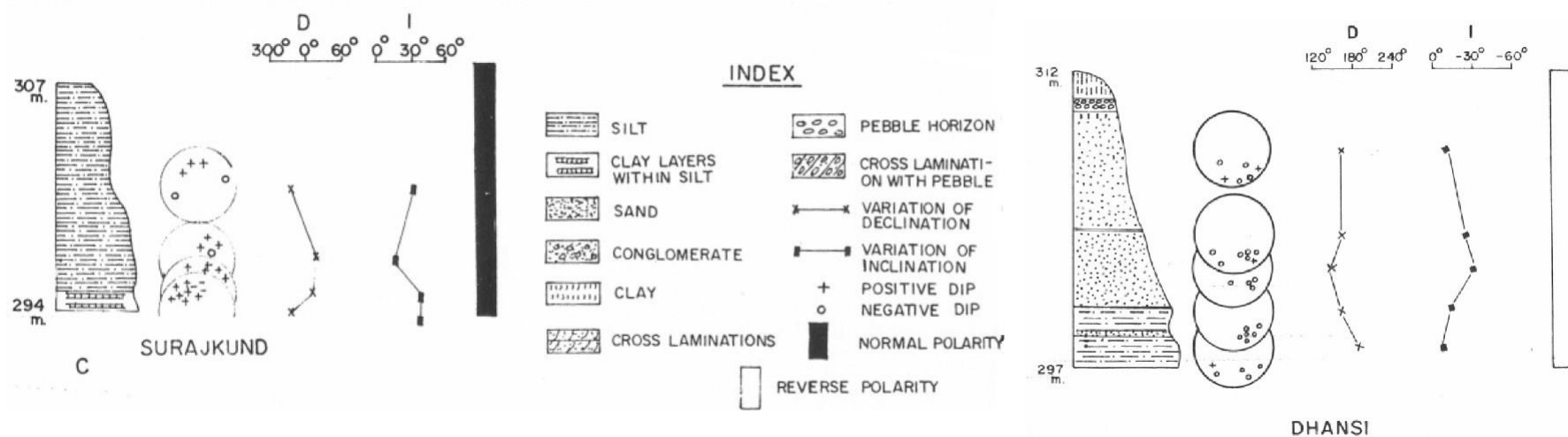
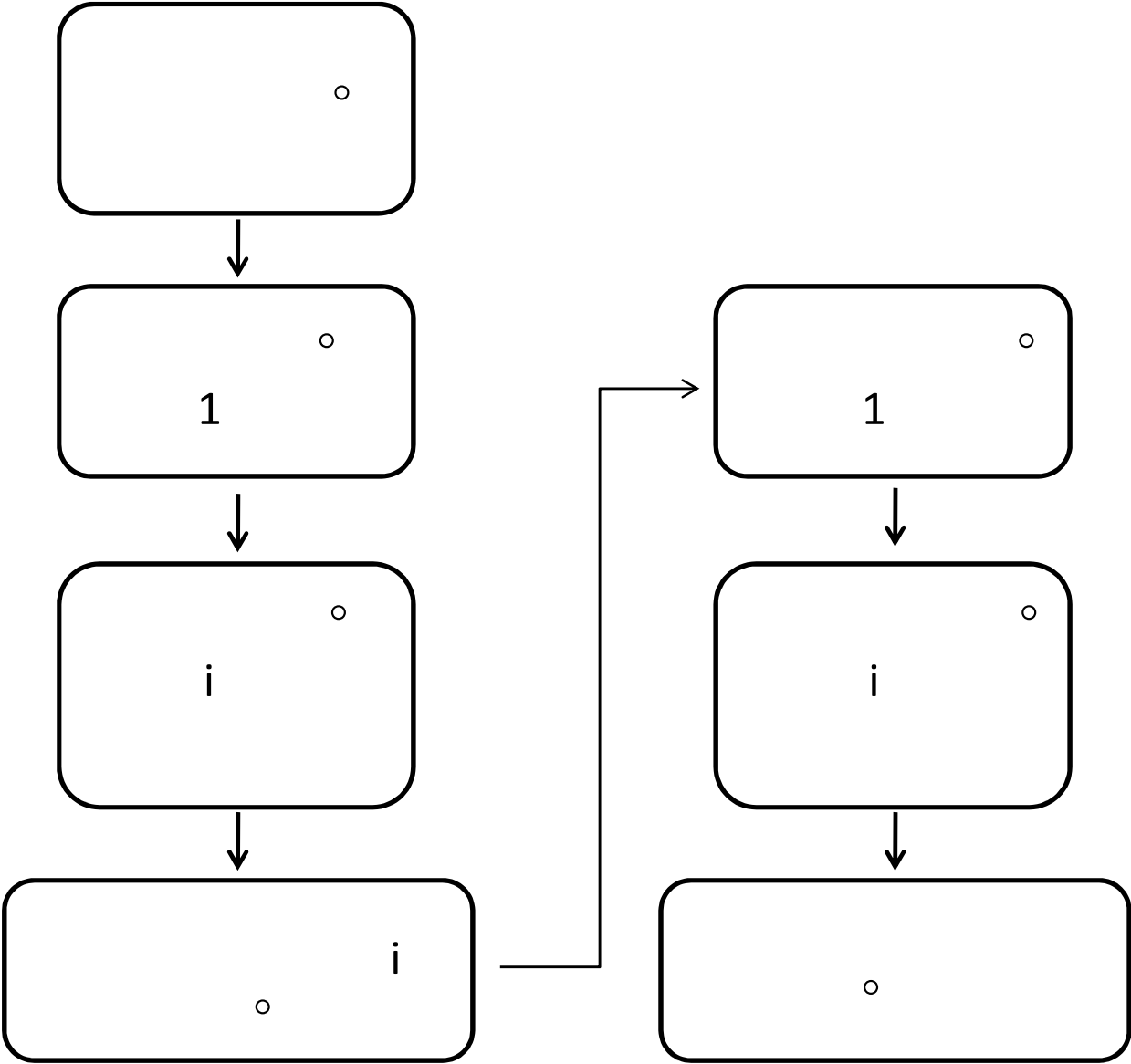


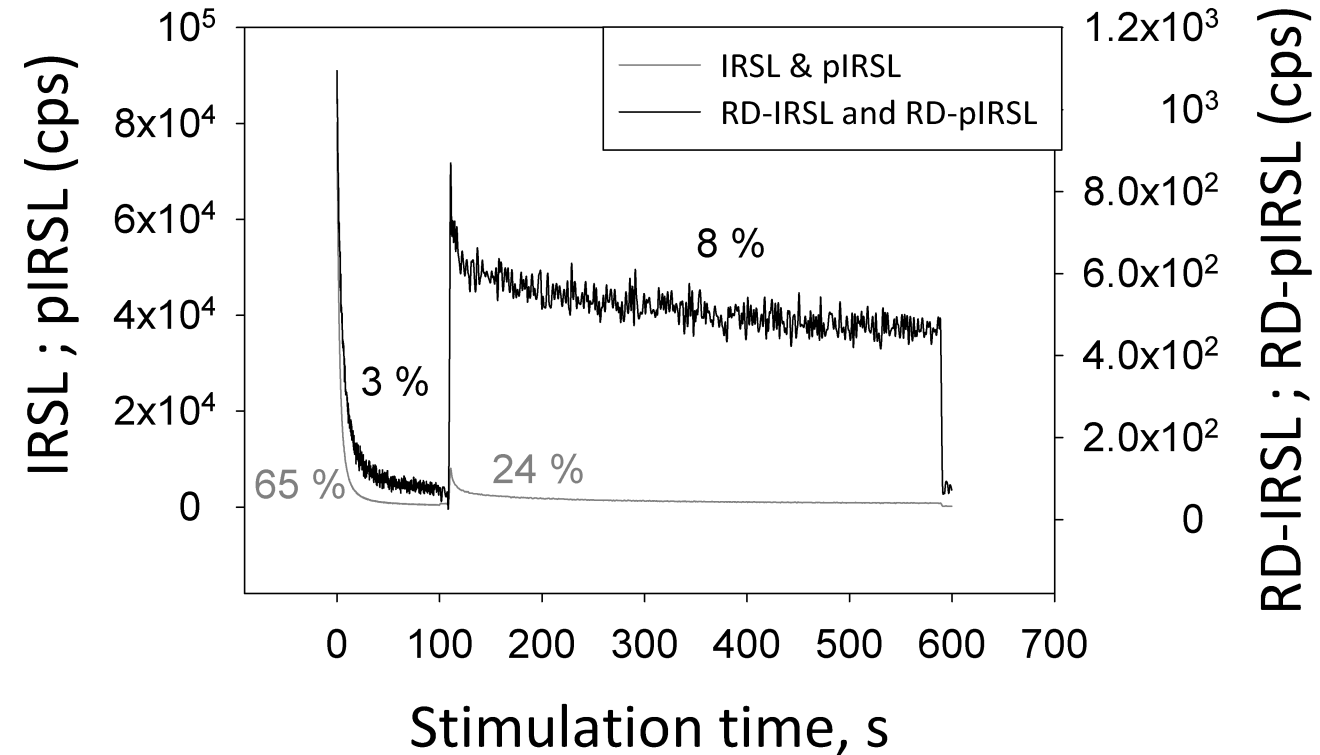


Fig.



Figure

Fig.3



Figure

Fig.  
Unbleached Dose, Gy

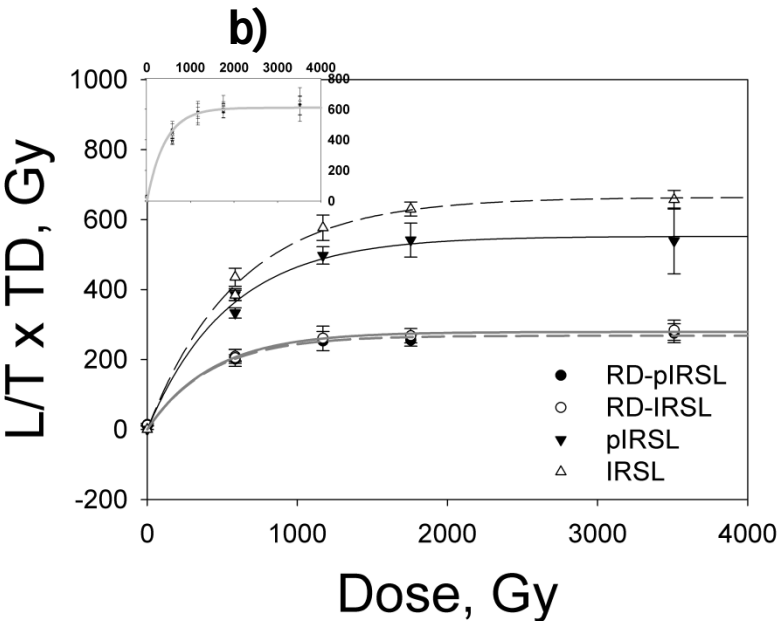
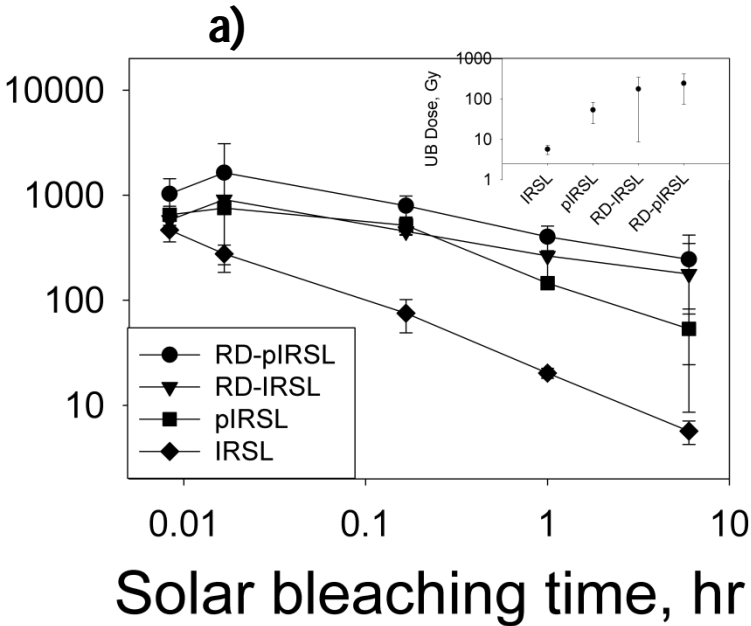
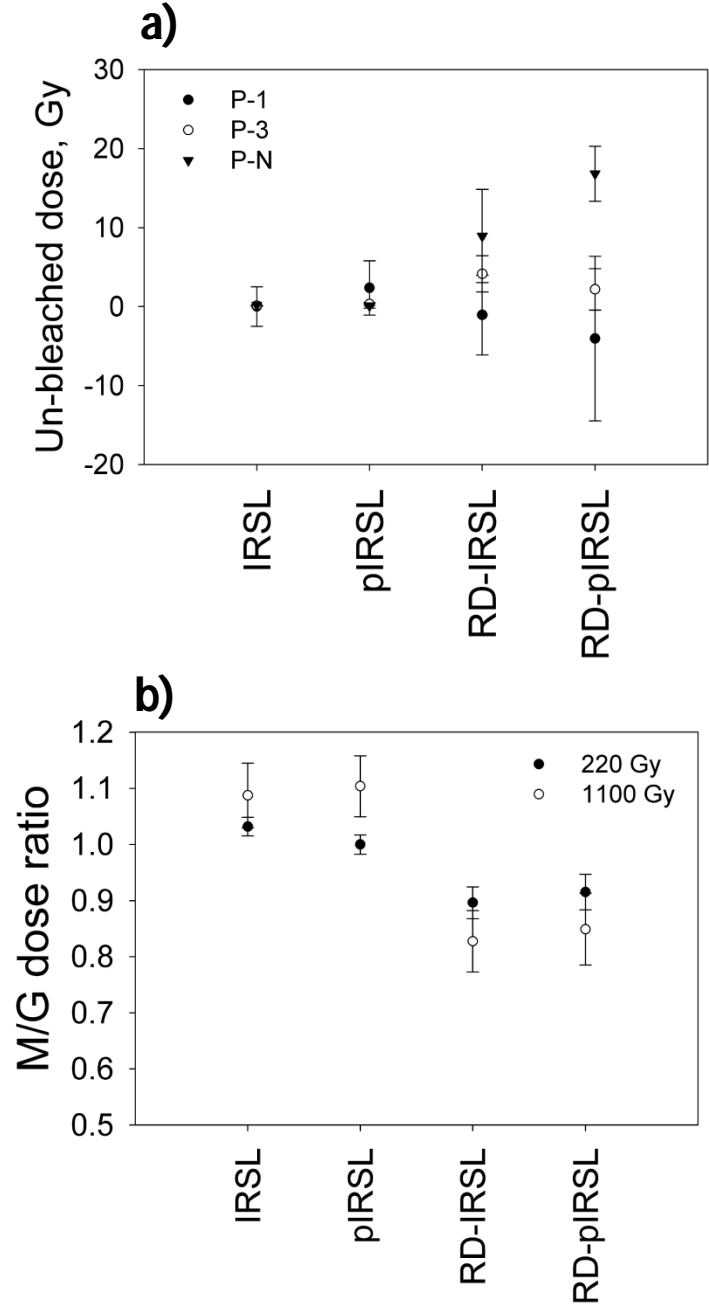


Fig.



Figure

Fig.

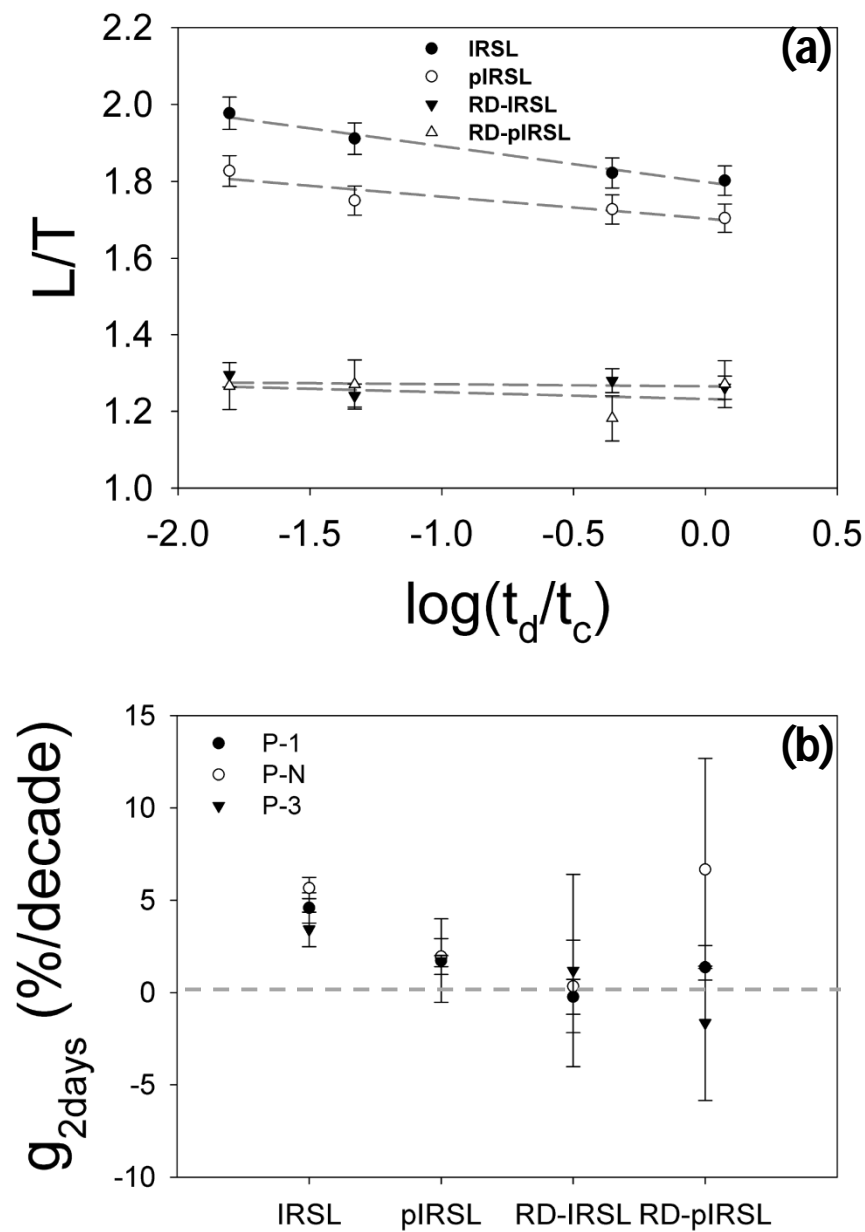
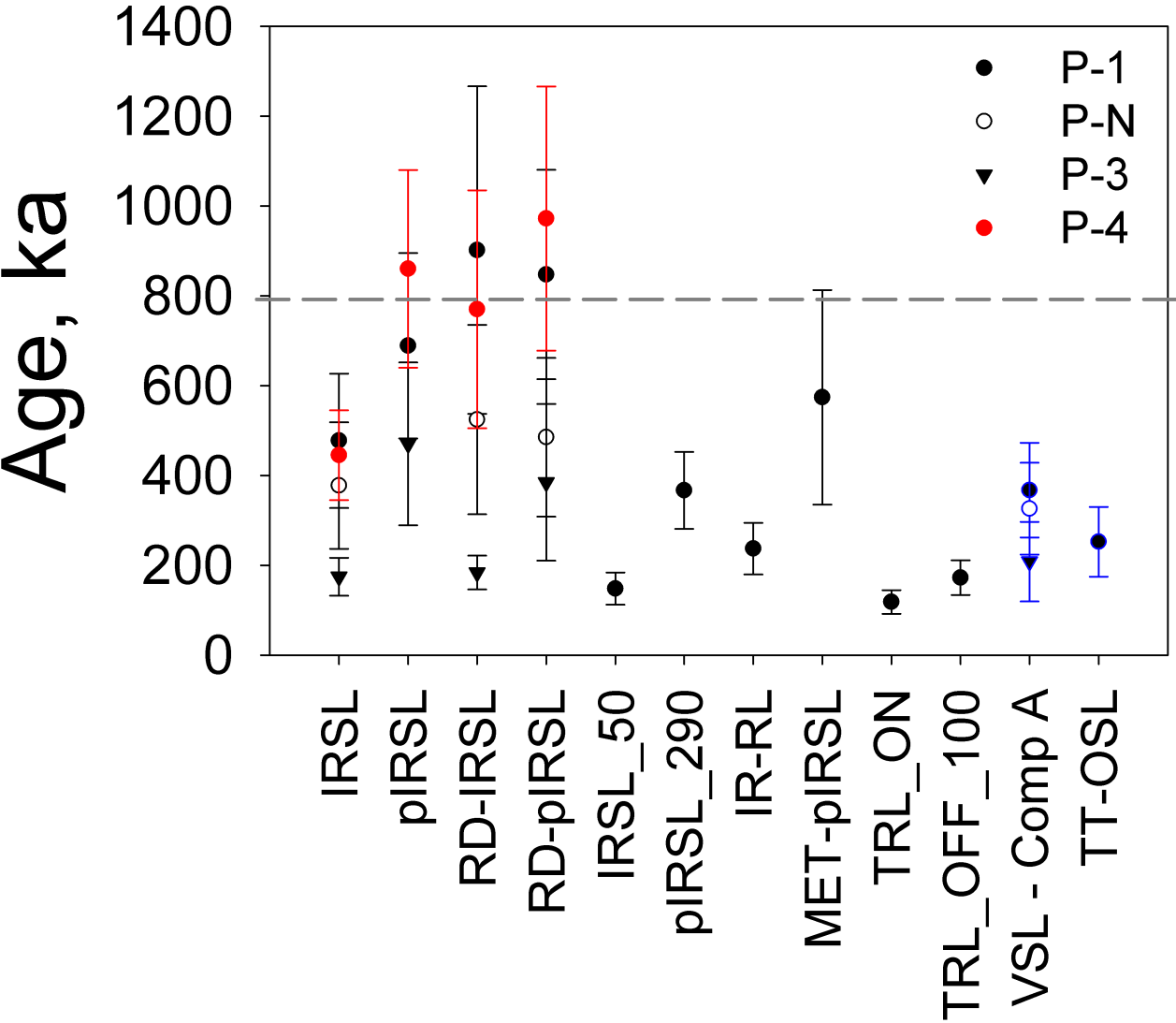


Fig. 7



**Table 1:** Measured parameters and estimated ages for the 4 samples of this study.

Sl. No.	Sample	Depth <sup>†</sup> (cm)	U (ppm)	Th (ppm)	K (%)	Dose Rate (Gy.ka <sup>-1</sup> )	Burial Dose (Gy)	Age (ka)
1.	DNS OSL P-1	100	1.2±1.1	5.6±3.3	0.8±0.2	2.4±0.5	2173±765	900±365
2	DNS OSL P-N	35	1.1±0.2	13.1±1.8	1.2±0.2	3.1±0.3	1625±635	520±210
3.	DNS OSL P-3	-100	2.5±1.0	15.0±3.2	1.1±0.2	3.6±0.4	662±114	184±38
4.	DNS OSL P-4	-210	0.3±1.0	4.8±3.0	0.7±0.2	1.9±0.4	1450±390	770±265

<sup>†</sup> Depth is calculated with respect to the artifact horizon. Artifact horizon is at 13 m from the top.

- Assumed water content and internal K concentration are  $5 \pm 2 \%$  ( $10 \pm 5 \%$  for DNS OSL P-3 and P-4) and  $13.5 \pm 0.5 \%$  respectively.
- Calculated mean cosmic dose rate was  $1.19 \pm 0.12 \mu\text{Gy.a}^{-1}$ .